

Cooperative Relative Pose Estimation to Aid Landing of an Unmanned Aerial Vehicle on a Moving Platform

Nikita Mishra¹, Anusna Chakraborty¹, Rajnikant Sharma¹, Kevin Brink²

Abstract—In this paper, we develop a method to estimate the relative position and relative heading of an Unmanned Aerial Vehicle (UAV) attempting to land on a moving platform using range-only measurements under GPS-denied conditions. Landing problems typically require precise estimation of relative position and heading, the proposed solution estimates relative pose between the platform (in this case a ship deck) and the landing multirotor. Vision-based landing techniques although accurate will fail under hostile weather conditions with the lack of Global Positioning System (GPS). This formulation investigates the effect on estimation quality when a single vehicle attempts to land using measurements from the ship only versus a team of multirotors assisting a vehicle to land on the ship. A multi-vehicle simulator has been developed in MATLAB/Simulink that facilitates testing our approaches. The simulation results clearly demonstrate the advantage of using a team for assisted landing rather than alone vehicle performing relative pose estimation using a limited range measurements.

Index Terms—Autonomous Vehicle landing, Extended Kalman Filter (EKF), GPS-denied navigation, relative navigation, Cooperative Localization.

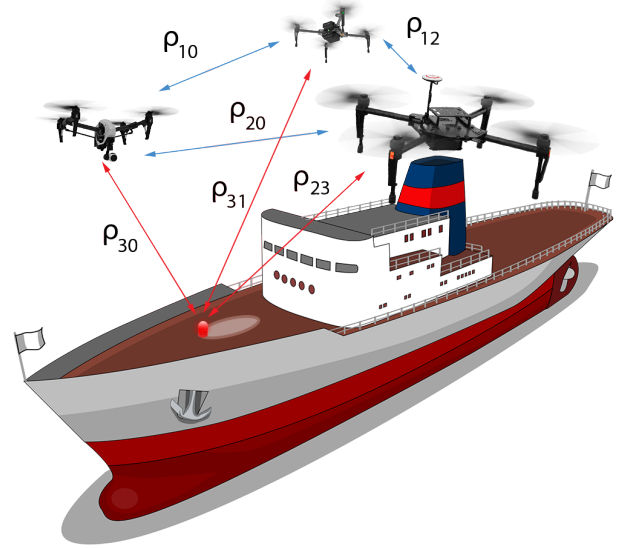


Fig. 1: Multirotor landing on ship using relative states coupled with cooperative localization

I. INTRODUCTION

Unmanned Vehicles (UVs), owing to their small size and versatile nature, find a number of civilian and military applications such as tracking lost objects [1], assessing damage due to natural disasters [2], package delivery using UAVs [3], and so on. In many of these scenarios UAVs are required to land on stationary or moving platforms such as a vehicle in motion, ship, or some building. Any scenario that involves landing would require a precise knowledge of the landing deck's position and the UAV's current position [4]. Currently, most landing mechanisms use image processing algorithms in addition to GPS measurements. In hostile conditions or disaster affected areas, GPS measurements may be unreliable (have a large uncertainty). Under such circumstances, vision-based landing techniques have been shown to be able to successfully land UAVs on moving platforms.

Most of the recent literature in GPS denied landing applications use various vision based techniques to aid a single vehicle to land on a fixed or moving platform. Lange *et. al* uses an optical flow technique to detect a suitable landing pad and then guide a multirotor to land in [5]. A feature-based image-matching algorithm has been performed in [6] to find landmarks (known points of interest) and then optical flow is used to safely land the UAV. Lee *et. al* used an image-based virtual servoing in [7] to track the platform and then uses an adaptive controller to land a Vertical Take Off and Landing (VTOL) vehicle on the moving platform. Sanchez *et.al* in [8] uses a downward facing camera to aid a VTOL UAV in landing on a ship deck. The ship deck is modelled accurately using the ship's equations of motion to replicate a ship's sinusoidal motion at sea. Wang and Bai implemented a multirotor landing on a moving platform using an ARdrone and a platform with a landing surface that emulates a ship's motion in [9]. This uses image processing algorithm to detect the landing symbol on the deck and then uses a PID controller to direct the multirotor to towards the landing pad. All of these techniques are based on vision-based approaches to assist in landing. At night time or in rough weather conditions, vision based landing algorithms will fail without any added sensor measurements. With a vision based approach, the vehicles have to maintain line-of-

¹ Nikita Mishra, Anusna Chakraborty and Rajnikant Sharma are with the Dept. Of Aerospace Engineering and Engineering Mechanics, University of Cincinnati email: sharmar7@ucmail.uc.edu

² Kevin M. Brink is with the Munitions Directorate, Air Force Research Laboratory, Eglin Air Force Base email: kevin.brink@us.af.mil

This work was funded by Air Force Research Laboratory through AFRL Grant FA8651-16-1-0001.

sight with the landing site which may be difficult if obstacles are present and may lead to poor estimation qualities from filter inconsistencies. In the absence of GPS, as global coordinates are unknown, we focus on a relative framework approach where all the states are estimated in the landing vehicle's frame. Relative pose and relative heading for a 2D case was estimated in [10] using range-only measurements. In this paper, we have extended the relative localization (RL) problem to a 3D framework that can estimate the relative pose and relative heading between the landing surface and UAV. Estimation using a single vehicle may render the filter unobservable if enough measurements are not present. Using multiple vehicles that cooperate among themselves to assist a single vehicle in landing has not been explored in the literature to the best of our knowledge. A team of vehicles for most UAV applications is preferred over a single one as it increases robustness and efficiency of the system. Cooperative localization occurs when multiple vehicles share their internal and external sensor information to improve the estimate for the group as a whole [11]–[13]. Most of the literature assumes the availability of known features that aid in estimation. However, when trying to land a multirotor on a vessel at sea, the terrain may not have any distinguishable features. In this paper, we leverage the strength of cooperative localization with 3D relative pose and heading estimation to provide accurate estimation using range-only measurements. Our main contributions can be summarized as (1) Develop equations of motion for a 3D relative pose and heading estimation. (2) Develop a cooperative relative estimation (CRL) framework that uses range measurements from assisting vehicles that aid the estimation quality of the UAV attempting to land on the ship.

II. PROBLEM FORMULATION

A. UAV Equations of Motion

Let us consider three multirotor UAVs and a ship as shown in Figure 1. We use $i = 0, 1, 2, 3$ index for the three UAVs and $i = 0$ for the vehicle that is landing. The 12-state equation of motion for the i^{th} UAV can be written as

$$\dot{p}_i = R_i V_i \quad (1)$$

$$\dot{V}_i = -(\Omega_i \times V_i) + g \begin{bmatrix} -\sin \theta_i \\ \cos \theta_i \sin \phi_i \\ \cos \theta_i \cos \phi_i \end{bmatrix} + \begin{bmatrix} 0 \\ 0 \\ -\frac{T_i}{m_i} \end{bmatrix} \quad (2)$$

$$\begin{bmatrix} \dot{\phi}_i \\ \dot{\theta}_i \\ \dot{\psi}_i \end{bmatrix} = \begin{bmatrix} 1 & \sin \phi_i \tan \theta_i & \cos \phi_i \tan \theta_i \\ 0 & \cos \phi_i & -\sin \phi_i \\ 0 & \frac{\sin \phi_i}{\cos \theta_i} & \frac{\cos \phi_i}{\cos \theta_i} \end{bmatrix} \Omega_i \quad (3)$$

$$\dot{\Omega}_i = J_i^{-1} \left(-\Omega_i \times J_i \Omega_i + \begin{bmatrix} \tau_{\phi_i} \\ \tau_{\theta_i} \\ \tau_{\psi_i} \end{bmatrix} \right) \quad (4)$$

where p_i is the position vector of the i^{th} UAV in north, east, and down (NED) coordinate frame. R_i is body to inertial frame rotation matrix written as

$$R_i = R(\psi_i)R(\theta_i)R(\phi_i) \quad (5)$$

$$\text{where } R(\psi_i) = \begin{bmatrix} \cos \psi_i & \sin \psi_i & 0 \\ -\sin \psi_i & \cos \psi_i & 0 \\ 0 & 0 & 1 \end{bmatrix}, \quad R(\theta_i) = \begin{bmatrix} \cos \theta_i & 0 & -\sin \theta_i \\ 0 & 1 & 0 \\ \sin \theta_i & 0 & \cos \theta_i \end{bmatrix} \quad R(\phi_i) = \begin{bmatrix} 1 & 0 & 0 \\ 0 & \cos \phi_i & \sin \phi_i \\ 0 & -\sin \phi_i & \cos \phi_i \end{bmatrix},$$

V_i is the velocity vector in the body frame, $[\phi_i, \theta_i, \psi_i]$ are the roll, pitch, and yaw angles (attitude) of the UAV, g is the acceleration due to gravity, Ω_i is the angular velocity vector in the body frame and is given as $[pp_i, q_i, r_i]^T$, J_i is the moment of inertia matrix, m_i is the mass of the UAV, T_i is the overall thrust generated by all the propellers, $\tau_{\phi_i}, \tau_{\theta_i}$, and τ_{ψ_i} are the torques in the body frame generated by all the propellers.

Most of the multirotor UAVs, as shown in Fig. 2, are equipped with autopilots with inbuilt attitude and velocity controller that takes body frame velocity V_i and angular velocity (yaw rate) r_i along the z -axis of the UAV as input and internally generate desired attitude, thrust, and torques to maintain the desired V_i and r_i . Therefore, to take into account the autopilot we will use the following reduced 4-state (position and heading) model for the i^{th} UAV.

$$\dot{p}_i = R_i V_i \quad (6)$$

$$\dot{\psi}_i = r_i. \quad (7)$$

It is important to note that for simplicity in this paper, we have used (6) and (7) to model the ship's motion. Detailed derivations of the equations of motion of a ship is done in [14]. Using (6) and (7), we derive the relative equations of motion in Section II-B.

B. Relative Equations of Motion

Since we are envisioning this operation to happen in GPS-denied environments inertial (NED) positions of the UAVs and ship are not available. Therefore it is important to estimate the relative position and relative heading between two vehicles. In this subsection we derive relative equations of motion in the body frame of the UAV ($i = 0$) that is landing. The relative position and relative heading between the i^{th} and j^{th} vehicle in i^{th} vehicle's body frame can be written as

$$p_{ji}^i = R_i^T (p_j - p_i) \quad (8)$$

$$\psi_{ji}^i = \psi_j - \psi_i \quad (9)$$

Differentiating (8) from both sides with respect to time, we get

$$\dot{p}_{ji}^i = \dot{R}_i^T (p_j - p_i) + R_i^T (\dot{p}_j - \dot{p}_i)$$

Substituting $\dot{R}_i = R_i S_i$ and using (6), we get

$$\dot{p}_{ji}^i = S_i^T R_i^T (p_j - p_i) + R_i^T (R_j V_j - R_i V_i)$$

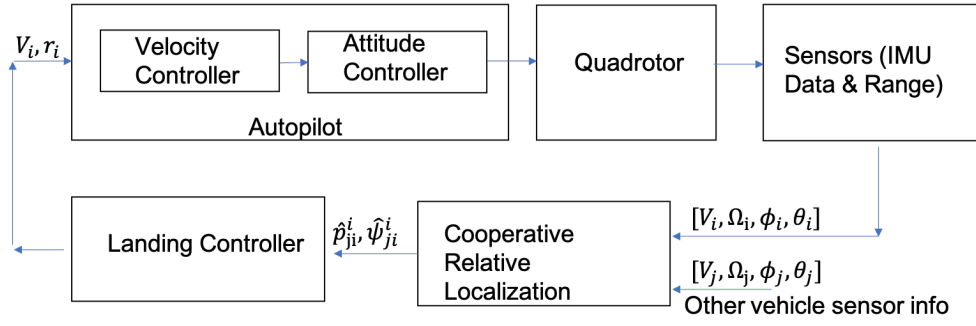


Fig. 2: Block Diagram representing the system architecture

where, $S_i = \begin{bmatrix} 0 & -r_i & q_i \\ r_i & 0 & -pp_i \\ -q_i & pp_i & 0 \end{bmatrix}$. Using (5) we can write the rotation matrix from j^{th} vehicle's body frame to i^{th} vehicle frame as

$$\begin{aligned} R_{ji} &= R_i^T R_j \\ &= R(\phi_i)^T R(\theta_i)^T R(\psi_i)^T R(\psi_j) R(\theta_j) R(\phi_j) \\ &= R(\phi_i)^T R(\theta_i)^T R(\psi_{ji}) R(\theta_j) R(\phi_j) \end{aligned} \quad (10)$$

where, $R(\psi_{ji}) = R(\psi_i)^T R(\psi_j)$. Differentiating (9), we can write the relative equation of motion between vehicle i and j in the i^{th} vehicle's body frame can be written as

$$\dot{x}_{ji}^i = f_{ji}(x_{ji}^i, u_i, u_j) = \begin{bmatrix} \dot{p}_{ji}^i \\ \dot{\psi}_{ji}^i \end{bmatrix} = \begin{bmatrix} S_i^T p_{ji}^i + R_{ji} V_j - V_i \\ r_j - r_i \end{bmatrix} \quad (11)$$

where, $x_{ji}^i = [(p_{ji}^i)^T \psi_{ji}^i]^T$ is the relative state vector, $u_i = [\Omega_i^T, V_i^T, \phi_i, \theta_i]^T$, and $u_j = [\Omega_j^T, V_j^T, \phi_j, \theta_j]^T$ are the control input vectors for the i^{th} and j^{th} vehicle respectively. Using (11), we formulate the cooperative relative estimation problem in Section III.

III. COOPERATIVE RELATIVE POSE ESTIMATION

In this section, we will develop a method to collaboratively estimate relative position and relative heading of all the vehicles (including ship) in the body frame of the UAV that is landing ($i = 0$). The joint relative state vector can be written as $x^i = [(x_{10}^0)^T, \dots, (x_{n0}^0)^T]^T$ for $i = 0$ and $j = 1, n$. The joint equation of the motion for three UAVs ($i = 0, 1, 2$) and the ship ($i = 3$) using (11) can be written as

$$\dot{x}^0 = f(x^0, u_0, u_{j=1,2,3}) = \begin{bmatrix} f_{10}(x_{10}^0, u_0, u_1) \\ f_{20}(x_{20}^0, u_0, u_2) \\ f_{30}(x_{30}^0, u_0, u_3) \end{bmatrix} \quad (12)$$

We assume that each vehicle including the ship is equipped with an IMU to measure and estimate its input vector $u_i = [\Omega_i^T, V_i^T, \phi_i, \theta_i]^T$ $i = 0, \dots, 3$. As shown in Fig. 2, each vehicle $j = 1, 2, 3$ communicates its u_j to the UAV ($i = 0$) that is landing to perform the relative pose estimation.

We also assume that all the vehicles are equipped with range sensors to measure range ρ_{ij} between two vehicles. For the landing scenario in this paper the UAV ($i = 0$) can measure range to other two UAVs ($j = 1, 2$) and the ship ($j = 3$).

$$\rho_{0j} = h_{0j}(x_{0j}^i) = \sqrt{(p_{0j}^0)^T p_{0j}^0}, \quad j = 1, \dots, 3 \quad (13)$$

If the landing UAV ($i = 0$) only uses the above measurements then it is like running three relative pose estimators due to lack of correlation between states. We also assume that other two UAVs can send their range measurements given below to the landing UAV.

$$\rho_{ij} = h_{ij}(x_{ij}^i) = \sqrt{(p_{0j}^i - p_{0j}^j)^T (p_{0j}^i - p_{0j}^j)}, \quad (14)$$

$$i = 1, 2, j = 2, 3 \quad (15)$$

The above measurements due to cross correlation will bring the aspect of cooperative relative localization in the picture. It will be shown in the results section that how these measurements improve the relative localization accuracy. We use an Extended Kalman Filter (EKF) to estimate joint relative position and relative vector \hat{x}^0 given $u_0, u_{j=1,2,3}$, and $\rho_{ij}, i = 0, 1, 2, j = 1, 2, 3$. The EKF-based Cooperative Relative Localization implementation is detailed in Algorithm 1.

where, σ_ρ is the measurement noise in the range sensor with zero mean gaussian noise and μ_ρ as standard deviation. Following Algorithm 1, cooperative localization technique can be used to jointly estimate the relative states of the multirotors in the system. These estimated states are fed to the controller in Section IV to generate the control inputs that finally enable the landing of the multirotor onto the ship deck.

IV. LANDING CONTROLLER

In this section, we derive a controller whose control objective is to drive relative position and heading of the ship ($i = 3$) $x_{30}^0 = [(p_{30}^0)^T \psi_{30}]^T$ in the UAV's body frame. We use a Proportional Integral (PI) control to compute the body frame velocity V_0 of the landing UAV.

Algorithm 1 EKF based Centralized Cooperative Localization using estimated relative pose and orientation

```

Initialize  $\hat{x}^k = x_0^k + \mathcal{N}(\mu, \sigma^2)$ .
for  $i$  in  $1 - N$  do ( $N$  - number of multirotors)
  for  $m$  in  $1 - NN$  do ( $NN$  - number of predictions before
  a measurement update)
     $\hat{x}^{k+} = \hat{x}^k + (\frac{T_s}{NN}) f(\hat{x}^k, u_0, u_{j=1,2,3})$  ( $k = 0$ )
     $A = \frac{\partial f}{\partial x^k} f(x^k, u_0, u_{j=1,2,3})$  (jacobian of eq (12))
     $P^+ = P^- + (\frac{T_s}{NN}) (AP + PA^T + Q)$ 
  end for
  if  $\rho_{0i}$  received then (range measurement between
  landing vehicle and  $i^{th}$  vehicle)
     $H_{0i} = \frac{\partial \rho_{0i}}{\partial x^k}$  (jacobian of (13))
     $L_{0i} = P^+ H_{0i}^T (\sigma_\rho^2 + H_{0i} P^+ H_{0i}^T)^{-1}$ 
     $\hat{x}^{k++} = \hat{x}^{k+} + L(\rho_{0i} - \hat{\rho}_{0i})$ 
     $P^{++} = (I - L_{0i} H_{0i}) P^+$ 
  end if
  for  $j$  in  $1 - N$  do
    if  $\rho_{ij}$  received and  $i \neq j$  then (range measurement
    between  $i^{th}$  and  $j^{th}$  vehicle)
       $H_{ij} = \frac{\partial \rho_{ij}}{\partial x^k}$  (jacobian of (15))
       $L_{ij} = P^+ H_{ij}^T (\sigma_\rho^2 + H_{ij} P^+ H_{ij}^T)^{-1}$ 
       $\hat{x}^{k++} = \hat{x}^{k++} + L(\rho_{ij} - \hat{\rho}_{ij})$ 
       $P^{++} = (I - L_{ij} H_{ij}) P^{++}$ 
    end if
  end for
end for

```

$$V_0 = R_{30} V_3 + K_p p_{30^0} + K_i \int_0^{T_s} p_{30^0}(\tau) d\tau \quad (16)$$

where, K_p and K_i are the diagonal proportional and integral gain matrices. The yaw rate r_0 of the landing UAV can be computed as

$$r_0 = r_1 + K_\psi \psi_{30}^0 \quad (17)$$

where, K_ψ is the proportional gain for the heading controller.

V. RESULTS

In this section, we present some simulation results that clearly demonstrate the advantage of cooperation among vehicles to assist landing in gps-denied conditions. Two cases are presented here based on the ship's trajectory. Figs 3- 6 represent the results when the ship is following a straight line and Figs 7- 10 represent the plots for ship moving in a circular trajectory. The simulation parameters used are listed as follows:

- Noise in range sensor = 0.2 m
- Noise in velocity = 0.2 m/s
- Noise in turn rates = 0.1 rad/s

Fig 3 represents the 3D inertial pose of the ship and the multirotors. Vehicles 2 and 3 are following circular

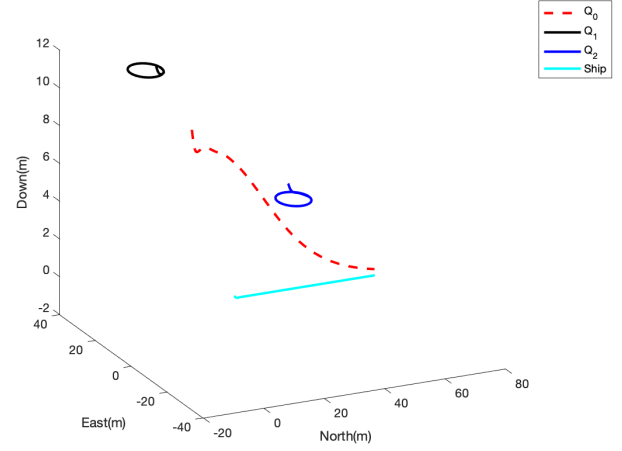


Fig. 3: Straight line - 3D Inertial frame trajectories of ship and all multirotors

trajectories while the ship is moving in a straight line. It is clear from the figure that the quad is able to estimate its pose and land on the ship using these estimated states. Fig 4 shows the comparison of the true and estimated states for the multirotor landing on the ship deck with just RL and with CRL. The states estimated using CRL follows the true trajectory very closely which is seen very clearly in the p_{z30} state. Although the estimation results using only relative localization between the ship and multirotor are decent, they have unwanted spikes as seen in the $\delta\psi_{30}$ plot. Such high fluctuations can generate very aggressive control commands which may disrupt the landing sequence. Figs 5 and 6 represent the error plots with 3σ bounds for the RL and CRL cases respectively. Even though using RL only, the states converge in the end, the filter is inconsistent in the beginning with higher uncertainties in the relative pose that may lead to failure in landing. The bounds with CRL on the other hand are much tighter and the error is much smoother resulting in precise landing.

Similarly, for the case where the ship is following a circular trajectory as seen in Fig 7, the relative pose estimated using only RL has more fluctuations specially at the beginning. This can be seen in Fig 8 which is similar to Fig 4. The spike in $\delta\psi_{30}$ is dangerous specially in the case when the ship's heading changes. Figs 9 and 10 corroborate with the results for the straight line case where the states estimated using only RL have high initial variations which renders the filter inconsistent. Cooperation among the vehicles and the ship helps reduce these unwanted alternations resulting in smoother and controlled landing. The simulation video for this case is available at the following link <https://youtu.be/kvCMPb5qxcM>.

VI. CONCLUSION AND FUTURE WORK

Based on the results in Section V, we can conclude that when the multirotors have the ability to measure range between each other, it improves the system estimates for all the

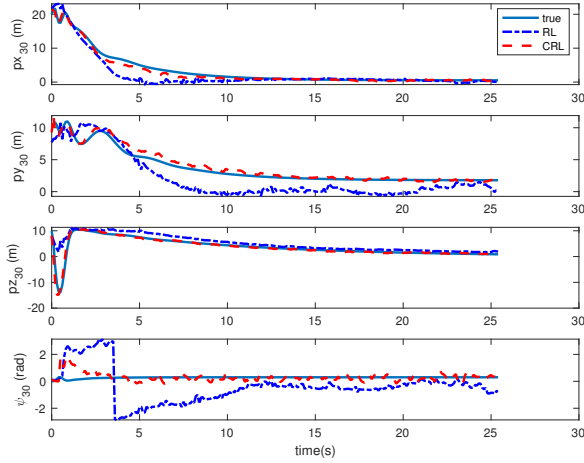


Fig. 4: Straight line - True vs Estimated states of ship with respect to the landing multirotor (true state - blue solid line, est. states with relative localization only - purple dotted line and est. states with with cooperative relative localization)

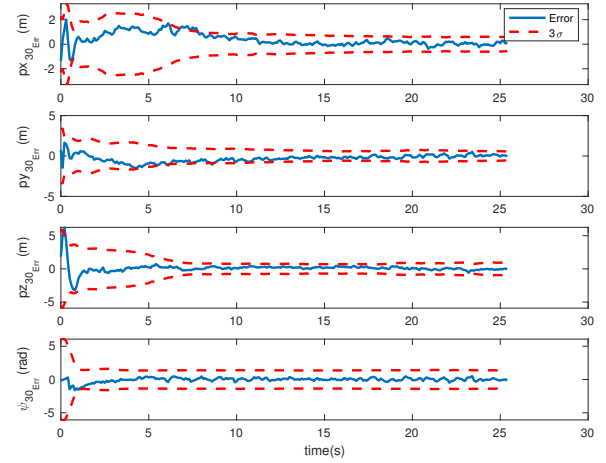


Fig. 6: Straight line - State errors with 3σ bounds with cooperative relative localization (error - blue solid line, 3σ - red dotted line)

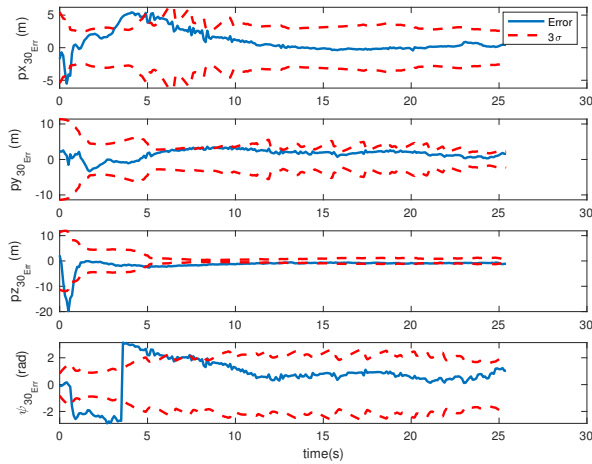


Fig. 5: Straight line - State errors with 3σ bounds with relative localization only (error - blue solid line, 3σ - red dotted line)

vehicles. Additional measurements also improve the system consistency as seen from the 3σ plots in Section V. Using relative cooperative localization with range measurements between agents, we can land a multirotor onto a moving platform in smooth and precise manner as well as estimate the relative position of all assisting vehicles and the

In this paper, we have considered a single range sensor on the ship deck. However, for large variations in the ship's motion, a single beacon for ranging may provide inaccurate information and so multiple range sensors can be placed on the deck. The performance of the filter depends on the system observability which will be analyzed for both cases. This analysis will be used to help in path planning of the supporting vehicles so as to increase observability

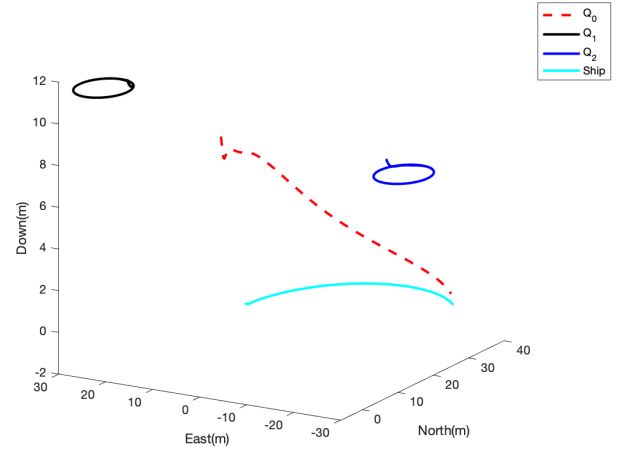


Fig. 7: Circle - 3D Inertial frame trajectories of ship and all multirotors

and decrease localization errors. An interesting extension of this work would be to explore ground vehicles moving on the ship deck while assisting multirotors to land. This might reduce the complexity of having to land all assisting vehicles when the system observability decreases. Hardware implementations demonstrating the advantage of CRL over RL will also be done as part in future for proof-of-concept.

REFERENCES

- [1] T. Furukawa, F. Bourgault, B. Lavis, and H. F. Durrant-Whyte, "Recursive bayesian search-and-tracking using coordinated uavs for lost targets," in *Robotics and Automation, 2006. ICRA 2006. Proceedings 2006 IEEE International Conference on*. IEEE, 2006, pp. 2521–2526.
- [2] P. Tatham, "An investigation into the suitability of the use of unmanned aerial vehicle systems (uavs) to support the initial needs assessment process in rapid onset humanitarian disasters," *International journal of risk assessment and management*, vol. 13, no. 1, pp. 60–78, 2009.

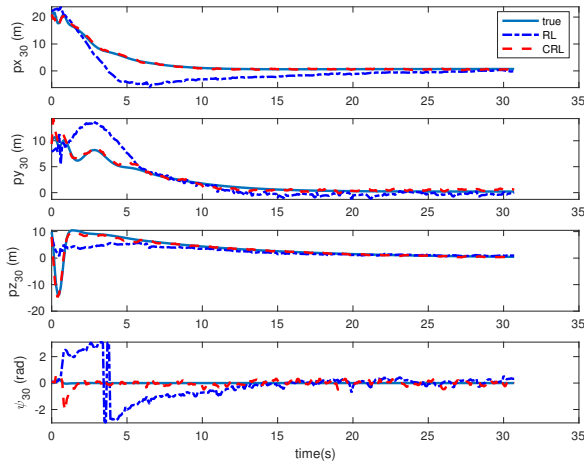


Fig. 8: Circle - True vs Estimated states of ship with respect to the landing multirotor (true state - blue solid line, est. states with relative localization only - purple dotted line and est. states with with cooperative relative localization)

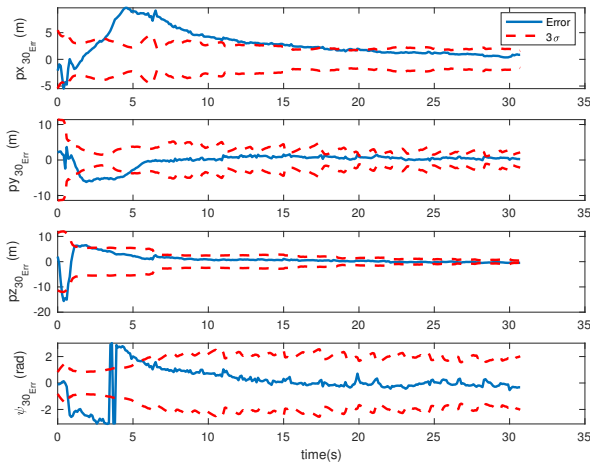


Fig. 9: Circle - State errors with 3σ bounds with relative localization only (error - blue solid line, 3σ - red dotted line)

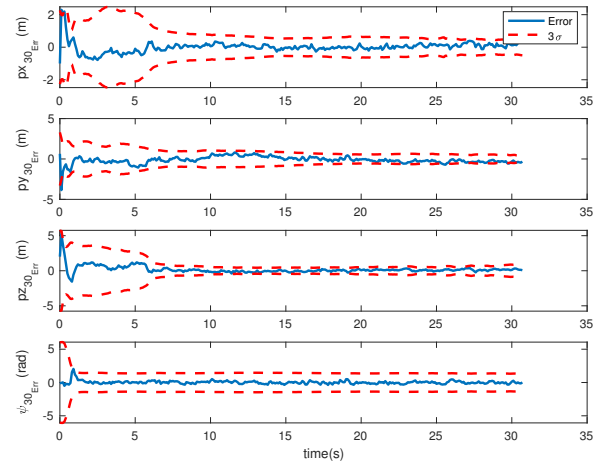


Fig. 10: Circle - State errors with 3σ bounds with cooperative relative localization (error - blue solid line, 3σ - red dotted line)

- [3] D. Haye Kesteloo, "Amazon's Prime Air may begin delivering packages by drone sooner than you think," <https://dronedj.com/2018/03/14/amazons-prime-air-drone-delivery/>, 2018, [Online; accessed 01-June-2018].
- [4] A. Cho, J. Kim, S. Lee, S. Choi, B. Lee, B. Kim, N. Park, D. Kim, and C. Kee, "Fully automatic taxiing, takeoff and landing of a uav using a single-antenna gps receiver only," in *Control, Automation and Systems, 2007. ICCAS'07. International Conference on*. IEEE, 2007, pp. 821–825.
- [5] S. Lange, N. Sunderhauf, and P. Protzel, "A vision based onboard approach for landing and position control of an autonomous multirotor uav in gps-denied environments," in *Advanced Robotics, 2009. ICAR 2009. International Conference on*. IEEE, 2009, pp. 1–6.
- [6] A. Cesetti, E. Frontoni, A. Mancini, P. Zingaretti, and S. Longhi, "A vision-based guidance system for uav navigation and safe landing using natural landmarks," *Journal of intelligent and robotic systems*, vol. 57, no. 1-4, p. 233, 2010.
- [7] D. Lee, T. Ryan, and H. J. Kim, "Autonomous landing of a vtol uav on a moving platform using image-based visual servoing," in *Robotics and Automation (ICRA), 2012 IEEE International Conference*

- on. IEEE, 2012, pp. 971–976.
- [8] J. L. Sanchez-Lopez, J. Pestana, S. Saripalli, and P. Campoy, "An approach toward visual autonomous ship board landing of a vtol uav," *Journal of Intelligent & Robotic Systems*, vol. 74, no. 1-2, pp. 113–127, 2014.
- [9] L. Wang and X. Bai, "Quadrotor autonomous approaching and landing on a vessel deck," *Journal of Intelligent & Robotic Systems*, pp. 1–19, 2017.
- [10] A. Chakraborty, K. Brink, R. Sharma, and L. Sahawneh, "Relative pose estimation using range-only measurements with large initial uncertainty," in *2018 Annual American Control Conference (ACC)*. IEEE, 2018, pp. 5055–5061.
- [11] A. Bahr, J. J. Leonard, and M. F. Fallon, "Cooperative localization for autonomous underwater vehicles," *The International Journal of Robotics Research*, vol. 28, no. 6, pp. 714–728, 2009.
- [12] R. Sharma, S. Quebe, R. W. Beard, and C. N. Taylor, "Bearing-only cooperative localization," *Journal of Intelligent & Robotic Systems*, vol. 72, no. 3-4, pp. 429–440, 2013.
- [13] A. Chakraborty, C. N. Taylor, R. Sharma, and K. M. Brink, "Cooperative localization for fixed wing unmanned aerial vehicles," in *Position, Location and Navigation Symposium (PLANS), 2016 IEEE/ION*. IEEE, 2016, pp. 106–117.
- [14] J. L. Sanchez-Lopez, S. Saripalli, P. Campoy, J. Pestana, and C. Fu, "Toward visual autonomous ship board landing of a vtol uav," in *Unmanned Aircraft Systems (ICUAS), 2013 International Conference on*. IEEE, 2013, pp. 779–788.